Published in final edited form as:
Biomacromolecules. 2007 September ; 8(9): 2781–2787. doi:10.1021/bm7004774.

Recognition of Conformational Changes in β-Lactoglobulin by Molecularly Imprinted Thin Films

Nicholas W. Turner[†,§], **Xiao Liu**[‡], **Sergey A. Piletsky**[§], **Vladimir Hlady**[†,*], and **David W. Britt**[‡,*]

†*Department of Bioengineering, University of Utah, Salt Lake City, Utah 84112*

‡*Department of Biological Engineering, Utah State University, 4105 Old Main Hill, Logan Utah 84322*

§*Cranfield Health, Cranfield University at Silsoe, Silsoe, Bedfordshire, MK45 4DT, U.K.*

Abstract

Pathogenesis in protein conformational diseases is initiated by changes in protein secondary structure. This molecular restructuring presents an opportunity for novel shape-based detection approaches, as protein molecular weight and chemistry are otherwise unaltered. Here we apply molecular imprinting to discriminate between distinct conformations of the model protein β-lactoglobulin (BLG). Thermal- and fluoro-alcohol-induced BLG isoforms were imprinted in thin films of 3-aminophenylboronic acid on quartz crystal microbalance chips. Enhanced rebinding of the template isoform was observed in all cases when compared to the binding of nontemplate isoforms over the concentration range of 1–100 μg mL^{-1}. Furthermore, it was observed that the greater the changes in the secondary structure of the template protein the lower the binding of native BLG challenges to the imprint, suggesting a strong steric influence in the recognition system. This feasibility study is a first demonstration of molecular imprints for recognition of distinct conformations of the same protein.

Introduction

Protein Conformation and Disease

Pathogenesis in the so-called “protein conformational diseases” is initiated by molecular-scale changes in the secondary structure of a specific protein, typically involving a transition from α-helix to β-sheet. These changes can elicit major shifts in the biological properties of the proteins, leading to phenomena such as insolubility, plaque formation, and resistance to proteases. Examples include Alzheimer’s,[1] Parkinson’s,[2] α1-antitrypsin deficiency,[3] the formation of cataracts,[4] and transmissible spongiform encephalopathies (TSEs) such as Creutzfeldt–Jakob disease (CJD), bovine spongiform encephalopathy (BSE), scrapie, and chronic wasting disease.[5–8] Studies of the α → β transitions and the properties of the distinct isoforms are therefore extremely important for the development of diagnostics as well as an elucidating the underlying mechanisms of these diseases.

β-Lactoglobulin Conformational Isomers

The whey protein β-lactoglobulin (BLG) has been studied extensively as a model protein exhibiting multiple stable conformations. BLG consists of 162 amino acid residues and has a M_W of about 18.3 kD and an isoelectric point at pH 5.1. BLG exhibits a dimeric structure at physiological pH, with each subunit consisting of nine antiparallel β-barrels and one small

*Corresponding authors. E-mail: dbritt@cc.usu.edu (D.W.B.); vladimir.hlady@utah.edu (V.H.). Tel.: +1 435 797 2158 (D.W.B.); +1 801 581 5042 (V.H.).

helix.[9] BLG also has a high α-helical propensity, and its ability to shift between conformational states is well documented.[10–12]

Thermal denaturation of BLG has been extensively investigated (with some differences in opinion).[13–18] Qi et al. have shown that upon heating BLG at pH 6.7, a progressive loss of β-sheet structure is observed, beginning below the denaturation temperature, with an abrupt loss of α-helical structure occurring above 65 °C.[18] The reversibility of BLG unfolding has also been investigated. Bhattacharjee and Das found that even at 85–90 °C the protein retains some of its folded structure, but upon cooling, the structure does not return to its native state. Using an extrinsic fluorescence probe they demonstrated the formation of deep hydrophobic clefts within the heat-treated protein, which are absent in native BLG.[19] This was further supported by Kim et al. using circular dichroism (CD) and interfacial measurements. [20] However, recent work using combined CD and FT-IR data indicates that the refolded form of BLG could be characterized as a molten globule state as it had native-like secondary structure and compromised tertiary structure.[13] This contradicts the work by Kim et al.[20] and Qi et al., [18] who suggested that upon cooling the secondary structure maintains a non-native state.

BLG conformational changes can also be induced by altering the solvent surrounding the protein. By reducing the water content of reverse micelles containing BLG a distorted β-sheet structure was reported.[21] Alcohol-induced stabilization of the BLG α-helical structure also occurs through a weakening of nonlocal hydrophobic interactions and an enhancement of local polar interactions.[22,23] This α-helix stabilizing effect is most prominent for 1,1,1,3,3,3-hexafluoroisopropanol (HFIP), followed by trifluoroethanol (TFE), with simpler alkyl-alcohols having a lesser influence. It is thought that the high polarity of fluoro-alcohols favors formation of micelle-like clusters that strongly affect the local solvent environment around the protein.[24,25]

Here, both thermal- and HFIP-induced BLG conformations are employed as distinct isoforms that are used as templates for forming synthetic recognition elements via molecular imprinting.

Molecular Imprinting

Molecularly imprinted polymers (MIPs) are made by forming a scaffold of functional monomers around a target template molecule followed by cross-linking. Upon template removal, the imprinted specific recognition sites are exposed in the polymer. Specific rebinding of the template occurs within these imprints, which are complementary to the template with respect to its surface properties, shape, and structure.[26,27] This technology has demonstrated potential in a variety of fields including separations,[28,29] sensing,[30–32] catalysis, [33,34] and drug delivery.[35]

Traditionally, molecular imprinting has been applied to small molecules such as amino acids, [36,37] toxins,[38–40] and drugs.[41–43] Selectivity between enantiomers[44,45] has been demonstrated, and affinities comparable to those obtained with antibodies have been achieved. [39] Although MIPs have been successfully developed against a wide range of small molecules, the imprinting of macromolecules, such as proteins, has proven more problematic. [46] Inherent technical problems include entrapment of the macromolecular template in the polymer matrix, poor mass transfer, low integrity of the polymer structure, restricted solvent compatibility, and the production of heterogeneous binding sites due to the geometric and chemical complexity of proteins.[47–49] Although surface imprinting approaches improve the mass transfer and reduce permanent entrapment of protein templates,[50–54] these methods also reduce the number of imprint sites, requiring sensitive techniques to detect rebinding events. Recent advances in the field suggest that these difficulties have been overcome and significant recognition of proteins can be achieved.[55,56]

Protein Imprinting in 3-Aminophenylboronic Acid

3-Aminophenylboronic acid (APBA) is an attractive matrix for protein imprinting, providing a mild aqueous environment during polymerization while offering a high number of favorable interactions with amino acids on the protein, as illustrated in Figure 1. Extending upon poly (APBA) as a matrix for small molecule imprinting,[57] Bossi et al. constructed poly(APBA) MIPs against a range of proteins in an effective microwell plate format.[58] The versatility of this polymer system was later demonstrated through the separation of diastereoisomers (ascorbic and isoascorbic acid) as well as protein separations (hemoglobin and glycosylated hemoglobin) in capillary electrophoresis (CE).[28]

Rick and Chou produced thin films of poly(APBA) on glass, imprinted with cytochrome *c* or lysozyme.[59,60] Using microcalorimetry they demonstrated imprint specificity through enthalpic changes associated with rebinding. Using quartz crystal microgravimetry (QCM) they further demonstrated the selectivity of cytochrome *c* and lysozyme MIPs for their respective templates. This work was recently extended to integration with an electrochemical sensor platform.[61]

Here we employ APBA as a protein imprint matrix for discriminating between native and thermal- or solvent-induced protein conformations of the model protein, bovine β-lactoglobulin. Circular dichroism is used here to confirm protein conformation changes. Protein (re)binding to imprinted and control poly(APBA) thin films is monitored using the quartz crystal microbalance. The surface properties of poly(APBA) at various stages of polymerization are further characterized using atomic force microscopy and sessile water drop contact angle analysis.

Materials and Methods

Materials

3-Aminophenylboronic acid (APBA), ammonium persulfate, 1,1,1,3,3,3-hexafluoroisopropanol (HFIP), acetic acid, and Tween 20 were purchased from Sigma (St. Louis, MO). All other chemicals and solvents were of commercial grade and used as received. Double-distilled deionized (DDI) water was prepared in-house. All reagents were stored at 4 °C and used at room temperature (22 °C). A running buffer of 50 mM sodium phosphate (pH 7) and a washing buffer of 3% acetic acid with 10 mM Tween 20 were prepared fresh for each experiment.

Protein

Bovine β-lactoglobulin (BLG) (95%) was purchased from Sigma (St. Louis, MO) and prepared as a 10 mg mL^{-1} stock solution in running buffer (50 mM sodium phosphate buffer, pH 7). This native form is referred to as N-BLG.

Heat-Treated Protein

A 10 mg mL^{-1} solution (in running buffer) of BLG was heated at 95 °C for 15 min in a water bath to induce an irreversible conformation change.[20] This isoform is referred to as heat-treated β-lactoglobulin (HT-BLG).

Fluoro-Alcohol-Exposed Protein

Fluoro-alcohol-induced isoforms were prepared by the addition of either 1% or 8% v/v of HFIP to 10 mg mL^{-1} solutions (in running buffer) of BLG. These are referred to as 1%HFIP-BLG and 8%HFIP-BLG, respectively.

Protein stock solutions were stored at 4 °C. For rebinding experiments protein solutions were serially diluted to the required concentration. For the HFIP–protein solutions, the desired HFIP/buffer solution ratios were maintained upon dilution.

Circular Dichroism

N-BLG and HT-BLG solutions (0.1 mg mL^{-1}) were prepared in running buffer. CD spectra of native, thermal-, and alcohol-induced BLG isoforms were measured with a CD spectropolarimeter (Aviv 62DS, Aviv, Japan). Sample volumes of 400 μL were placed in a 0.1 cm path length quartz cuvette, and spectra were collected by averaging five scans at 0.5 nm s^{-1} over the wavelength range of 300–190 nm, with background subtraction using protein-free solutions. These results are presented in terms of mean residual, or molar, ellipticity (Φ) in the units of mdeg cm^2 $dmol^{-1}$.

Polymer Preparation

QCM crystals (5 MHz Au/Ti, Stanford Research Systems) were cleaned with ethanol, followed by etching with oxygen plasma (O_2, 200 mtorr, 50 W, 1 min) in a plasma chamber (Plasmod, Tegal Corp.) resulting in a fully water-wettable surface, as confirmed by contact angle measurements (VCA Optima, AST Products,).

General protocols for imprinting of proteins within poly(APBA) matrixes have been described previously.[58,60] Briefly, nonimprinted films were formed as follows. Solutions of monomer, APBA (100 mM in buffer), and initiator, ammonium persulfate (50 mM in buffer), were prepared. Equal volumes were placed in glass vials followed by thorough mixing. Then, 50 μL aliquots were spread on QCM crystals, ensuring that the entire surface was covered within 30 s of the initial mixing.

Protein MIPs were prepared by adding the template protein to the 100 mM APBA solution at a concentration of 1 mg mL^{-1} and left to stand for 20 min. Next, an equal volume of the 50 mM ammonium persulfate initiator was added, yielding a final protein concentration of 0.5 mg mL^{-1}. For the imprinting of 1%HFIP-BLG and 8%HFIP-BLG, the 50 mM ammonium persulfate solution contained the appropriate fraction of HFIP. Imprinted polymer films were prepared on the surface of QCM crystals in the same manner as the nonimprinted films.

Polymer films were left to cure at room temperature in a covered Petri dish for 90 min followed by repeated washing with copious amounts of water and washing buffer (3% acetic acid containing 10 mM Tween 20) to remove weakly bound polymer/template. Following a final water rinse, the modified QCM chips were stored at 4 °C in 50 mM sodium phosphate buffer, pH 7.

Polymer Growth, Washing, and Surface Analysis

The polymerization process and integrity of the thin polymer films were further analyzed using atomic force microscopy (AFM) and water contact angle. At set time intervals the polymerization was stopped, and the polymers were washed as previously described. The films were dried in air, and the surface topology was analyzed using a Bioscope AFM with an NSIIIa controller (Digital Instruments, Inc.) in tapping mode with NSC-12 tips (Mikromash, Inc.). All samples were imaged between 1 × 1 μm^2 and 50 × 50 μm^2 and at several rotations. The rms roughness was calculated from 1 × 1 μm^2 images. Water contact angle measurements (VCA Optima, AST Products) were performed on the same films using 1 μL sessile drops of double-distilled water.

Microgravimetric Analysis of Protein Binding to APBA Layers

Protein adsorption to the blank and MIP poly(APBA) films was monitored using a 5 MHz quartz crystal microbalance (QCM200, Stanford Research Systems). The modified QCM chips were maintained hydrated during mounting in the QCM flowcell. Protein and rinse buffers were introduced using a gravity-driven flow setup designed to maintain a uniform hydrostatic pressure on the QCM chip.

The modified QCM chip was first stabilized in running buffer (50 mM sodium phosphate, pH 7) by passing several sample volumes from the feed reservoir. This was continued until the system reached equilibrium, indicated by frequency changes of less than 0.1 MHz upon running buffer exchanges. After recording a baseline signal for several minutes, the feed reservoir was filled with a protein solution, which was then passed through the flowcell. The flow was immediately stopped by a valve located on the downstream side and positioned at the same height as the flowcell, and the rinse reservoir was refilled. This careful placement of the flow control valve combined with refilling of the open rinse reservoir ensured a constant hydrostatic pressure on the QCM chip during measurements. Protein adsorption was then allowed to proceed under hydrostatic conditions until the QCM signal reached equilibrium. This titration process was repeated over the concentration range of 0.001–0.1 mg mL^{-1}. For experiments requiring HFIP, the system was pre-equilibrated using a 1% v/v HFIP solution. Binding isotherms are presented as normalized frequency changes plotted against bulk protein concentration on a logarithmic scale. It was assumed that polymer layers are rigid, and therefore, the Sauerbrey equation can be applied.

Results and Discussion

Formation of Polymers on Sensor Surfaces

The evolution of imprinted and nonimprinted poly(APBA) films was characterized using AFM and contact angle analysis. AFM images of imprinted films where polymerization was quenched by washing at 2, 10, 30, 60, and 120 min are presented in Figure 2.

AFM reveals discrete poly(APBA) islands (2 min), which begin to coalesce at 10 min polymerization time. By 30 min a confluent, but rough, film has formed. After 60 min the gross morphology did not appear to change, suggesting there was a limit to the thickness of the layer remaining post washing/rinsing. The morphology shown in these latter images is consistent with that obtained by Rick and Chou who analyzed confluent poly(APBA) layers before and after washing.[59]

From the images in Figure 2 the surface roughness of each sample was calculated and is presented along with the corresponding water contact angle in Figure 3. The water contact angle and rms data exhibit similar trends that indicate the polymerization results in a near complete coverage of the gold surface within 10 min, with the remainder of the surface filled in by 60 min. AFM analysis of the polymer measured the thickness of the APBA layers with respect to the underlying substrate to ~90–100 nm, consistent across all samples.

Similar trends were observed for blank poly(APBA) layers (data not shown), suggesting that the presence of protein does not significantly affect the growth of the polymer. This was also observed in SPR polymerization kinetics (data not shown). It was also noted that the addition of Tween 20 significantly slowed the polymerization/deposition rate (data not shown). In previous work Tween 20 had been used to suppress nonspecific interactions, during polymer formation and protein rebinding.[58,60] However, for these experiments we chose to omit this. This was done to avoid any potentially adverse effect on the formation of the polymer layer during polymerization and to ensure the interactions between polymer and template protein were maximized, as our different targets are similar in nature. More importantly, the presence

of a surfactant will potentially interfere with the minor protein conformational changes induced here.

(Re)binding of Native BLG to Imprinted and Blank Poly-(APBA)

Films prepared in the presence of native BLG (N-BLG) and the corresponding nonimprinted films were challenged with N-BLG to assess the imprinting effect versus nonspecific binding. Figure 4 shows a slightly enhanced rebinding of N-BLG to its imprinted film (closed squares) versus adsorption in the nonimprinted control (open squares). This suggests an imprinting effect, attributed to the formation of BLG-specific binding pockets within the poly(APBA) film. A two-factor ANOVA was performed on the two sets of data, giving a *p*-value of 0.00164 indicating that the observed differences are significant. The high nonspecific binding, as shown by the interaction between N-BLG and nonimprinted films, was attributed to the absence of a blocking agent during the rebinding process. Previous poly(APBA) protein imprinting employed Tween 20 to minimize nonspecific interactions between polymer and proteins.[58, 60] However, for the reasons noted above, surfactant was omitted here. This resulted in a lower observed contrast between imprint and control when compared to previous measurements of protein/poly(APBA) interactions obtained using QCM.[60]

Demonstration of Conformational Changes Using Circular Dichroism

To test conformational specificity, poly(APBA) films were imprinted with distinct BLG isoforms and cross-challenged. Figure 5 presents the CD spectra of N-BLG and thermal- and alcohol-induced isoforms. HT-BLG (spectrum 2, Figure 5) exhibited changes relative to the native protein (spectrum 1, Figure 5), which suggests that an increase in α-helix structure has occurred (indicated by a more pronounced minimum in ellipticity at 208 nm). This conclusion is supported by previously published work showing altered BLG secondary structure on heating, the extent of the change being dependent on the pH, temperature, and duration.[18, 20] The thermally induced conformational change is irreversible over several days,[19] presenting an ideal situation in the context of this work as it provided two stable, but distinct, protein conformations under the same environmental conditions.

A second approach to inducing BLG conformational changes was to add HFIP to the BLG solutions. Fluoro-alcohols are known to dramatically alter the secondary structures of proteins, and in the case of BLG shift the predominately β-sheet conformation toward an β-helical structure. Of the fluoro-alcohols, HFIP has been shown to be one of the strongest producers of this phenomenon.[25] The addition of 1% v/v HFIP to the protein solution shifted the CD spectrum downward slightly (spectrum 3, Figure 5), which probably represents an initial change into new secondary structure. This shift continues toward a state with high α-helical character upon addition of higher concentrations of HFIP (see Figure 8).

Imprinting of Alternate Conformations of BLG in APBA Matrix

The HT-BLG isoform and native (N-BLG) were both imprinted in the poly(APBA) matrix using the same protocol. After washing to remove the original template proteins, the imprints were challenged with the native and altered BLG, using the QCM to measure affinity of the protein to the immobilized films.

Figure 6A shows the rebinding of N-BLG to films imprinted with N-BLG and binding to control films imprinted with HT-BLG. In support of conformation-specific imprinting, it is seen that the N-BLG MIPs bound more of the N-BLG isoform than did MIPs imprinted with the heat-treated isoform. As further evidence of conformation selectivity, when the challenger protein is switched to HT-BLG (Figure 6B), the adsorption trend is reversed. In this case HT-BLG showed greater binding to the HT-BLG-imprinted films than to noncomplimentary films imprinted with the native protein. To our knowledge, this is the first demonstration of the

selective recognition of different conformational isomers of proteins by imprinted polymer films.

To further test this selectivity, we investigated imprints of another system. HFIP-induced conformational changes were formed and tested against native protein, and vice versa. HFIP (1% v/v) was added to the protein solution used for imprinting, allowing 20 min for the protein and fluoro-alcohol to interact before the initiator was added. Imprinted films were prepared using this isoform and the native form as a control, following the same protocol as that described above. Once the template proteins were removed, the imprints were challenged with both N-BLG and HFIP-BLG.

Although it was possible to keep the buffer solutions identical when comparing binding affinities of HT-BLG with N-BLG, for the HFIP-BLG isoform the running and rinse buffers contained 1% HFIP. Before the addition of any protein, the QCM was stabilized in this solvent mixture. The presence of HFIP in the running solutions resulted in a slight change (~2 Hz) in the frequency recorded by the QCM, relative to that of neat buffer, as a result of a slight increase in the density of the solution. Higher concentrations of HFIP, shown to produce greater conformational changes in the protein, could not be used as they had a detrimental effect on the stability of the QCM (data not shown). However, as will be shown later, it was possible to form poly(APBA) MIPs in the presence of up to 8% HFIP, allowing the MIP selectivity to be tested against native BLG in the QCM.

Figure 7A shows the binding of N-BLG to N-BLG MIPs and nonspecific binding to 1%HFIP-BLG MIPs. The N-BLG-imprinted film showed greater affinity for N-BLG than the film imprinted with the fluoro-alcohol-induced isoform. The complementary experiment mirrored this, with preferential binding of the template 1%HFIP-BLG to the 1%HFIP-BLG-imprinted film than to that imprinted with N-BLG (Figure 7B). These results parallel the binding trends observed for the thermally induced conformers, demonstrating that BLG conformers derived from two distinct mechanisms can be imprinted and discriminated from native BLG through molecular imprinting.

In both these cases, where pairs of isoforms were used to challenge their corresponding pairs of imprinted films, greater binding of the templates to their respective imprints was seen. This suggests that specific imprints for each isoform were created, and these possess enhanced affinity for the conformational form of the protein used as template. As the underlying chemistry of the polymer films is the same in all experiments, recognition is expected to arise from a combination of steric factors and from the positioning of complementary functionality within the imprint sites. In order to study the importance of imprint shape on recognition, a range of isoforms, prepared by the action of the fluoro-alcohol HFIP on BLG, were imprinted, and the polymers were challenged with the native protein. We hypothesize that the greater the conformational change shown by the template isoform, the lower should be the binding of the native protein to this MIP.

Figure 8 shows the CD spectra obtained for these isoforms. Curves 1 and 2 are the native and 1% HFIP isoforms described above. A range of HFIP concentrations was tested for their effect on the conformation of BLG, as assessed from their CD spectra (data not shown). The greatest conformational change, observed as a large increase in α-helical character (at 208 and 222 nm), was generated with 8% HFIP (curve 3, Figure 8). These three conformations were then imprinted in the poly(APBA) matrix, as described above, and the films were challenged with the native isoform (N-BLG) in 50 mM phosphate buffer, pH 7. The rebinding data is presented in Figure 9. The observed binding was greatest between N-BLG and the N-BLG-imprinted film, less binding was seen with the 1%HFIP-BLG-imprinted polymer, and the least with the 8%HFIP-BLG-imprinted film. The affinity of N-BLG for the imprinted films was therefore

observed to decrease as the extent of conformational change of the template protein was increased, as illustrated schematically in Figure 10.

Conclusions

Different isoforms of BLG were created by thermal treatment and by the use of different concentrations of a fluoro-alcohol. APBA-derived polymer films were imprinted with these different isoforms of BLG and tested against the same set of isoforms. The production of these films was monitored by AFM and water contact angle measurements. It was found that growth in all polymers was comparable. Using QCM to monitor protein adsorption, the greatest affinity was observed for rebinding of the isoforms to their own imprints, demonstrating the importance of steric contributions to the creation of protein-imprinted cavities. The results presented here are modest in terms of the magnitude of their effect, when compared to the recognition obtained by certain recent advances in protein imprinting.[55,56,61] They however demonstrate the validity of the molecular imprinting technique for the detection of *distinct* conformations of the same protein. This is a step forward from recognition between different proteins and, despite the modest selectivity, demonstrates the flexibility of the molecular imprinting technique. The clear importance of the steric contribution to recognition suggests that imprinting could be used for the creation of materials capable of differentiating between conformers in systems that exhibit major changes in conformation. These could include proteins such as scrapie native prion PrPc and its pathogenic PrPSc form, which differ by a 40% increase in β-sheet and ~15% decrease in α-helix in the latter over the former.[62,63] Protein conformational imprinting may thus offer a unique means to detect non-native pathogenic proteins in situ. Greater discrimination may be attainable by using more complex imprint matrixes as well as incorporation of blocking agents to reduce nonspecific binding outside of the imprint sites.

Acknowledgment

N.W.T. thanks Dr. Mike Whitcombe, Ned Ashby, and Dr. Michael Kay for insightful comments. N.W.T., V.H., and D.W.B. acknowledge funding from the National Research Initiative of the USDA Cooperative State Research, Education and Extension Service, Grant No. 2005-35603-15829. S.A.P. acknowledges with gratitude receiving a Royal Society-Wolfson Research Merit Award.

References and Notes

1. Clippingdale AB, Wade JD, Barrow CJ. J. Pept. Sci 2001;7:227–249. [PubMed: 11428545]
2. Galvin JE, Lee MY, Trojanowski JQ. Arch. Neurol 2001;58:186–190. [PubMed: 11176955]
3. Carrell RW, Lomas DA, Sidhar SK, Foreman RC. Chest 1996;110:243S–247S. [PubMed: 8989158]
4. Pande A, Pande J, Asherie N, Lomakin A, Ogun O, King J, Benedek G. Proc. Natl. Acad. Sci. U.S.A 2001;98:6116–6120. [PubMed: 11371638]
5. Collinge J. Annu. Rev. Neurosci 2001;24:519–550. [PubMed: 11283320]
6. Soto C, Estrada L, Castilla J. Trends Biochem. Sci 2006;31:150–155. [PubMed: 16473510]
7. Dobson CM. Trends Biochem. Sci 1999;24:329–332. [PubMed: 10470028]
8. Carrell RW, Lomas DA. Lancet 1997;350:134–138. [PubMed: 9228977]
9. Forge V, Hoshino M, Kuwata K, Arai M, Kuwajima K, Batt CA, Goto Y. J. Mol. Biol 2000;296:1039–1051. [PubMed: 10686102]
10. Nishikawa K, Noguchi T. Methods Enzymol 1991;202:21–24.
11. Kuroda Y, Hamada D, Tanaka T, Goto Y. Folding Des 1996;1:243–251.
12. Kuwata K, Shastry R, Cheng H, Hoshino M, Batt CA, Goto Y, Roder H. Nat. Struct. Mol. Biol 2001;8:151–155.
13. Bhattacharjee C, Saha S, Biswas A, Kundu M, Ghosh L, Das KP. Protein J 2005;24:27–35. [PubMed: 15756815]
14. Dufour E, Haertle T. Int. J. Biol. Macromol 1993;15:293–297. [PubMed: 8251444]

15. Dufour E, Genot C, Haertle T. Biochim. Biophys. Acta 1994;1205:105–112. [PubMed: 8142474]
16. Kella NKD, Kinsella JE. Biochem. J 1988;255:113–118. [PubMed: 3196307]
17. Laligant A, Dumay E, Casas Valencia C, Cuq JL, Cheftel JC. J. Agric. Food Chem 1991;39:2147–2155.
18. Qi XL, Holt C, Mcnulty D, Clarke DT, Brownlows S, Jones GR. Biochem. J 1997;324:341–346. [PubMed: 9164875]
19. Bhattacharjee C, Das KP. Eur. J. Biochem 2000;267:3957–3964. [PubMed: 10866794]
20. Kim DA, Cornec M, Narsimhan G. J. Colloid Interface Sci 2005;285:100–109. [PubMed: 15797402]
21. Andrade SM, Carvalho TI, Viseu MI, Costa SMB. Eur. J. Biochem 2004;271:724–744. [PubMed: 14764088]
22. Shiraki K, Nishikawa K, Goto Y. J. Mol. Biol 1995;245:180–194. [PubMed: 7799434]
23. Thomas PD, Dill KA. Protein Sci 1993;2:2050–2065. [PubMed: 8298455]
24. Gast K, Siemer A, Zirwer D, Damaschun G. Eur. Biophys. J 2001;30:273–283. [PubMed: 11548130]
25. Hirota K, Mizuno K, Goto M. Protein Sci 1997;6:416–421. [PubMed: 9041644]
26. Wulff G. Angew. Chem., Int. Ed 1995;34:1812–1832.
27. Sellergren, B. Molecularly Imprinted Polymers: Man-Made Mimics of Antibodies and Their Applications in Analytical Chemistry. Sellergren, B., editor. Vol. Vol. 23. Amsterdam: Elsevier; 2001. p. 113-183.
28. Bossi A, Castelletti L, Piletsky SA, Turner AP, Righetti PG. J. Chromatogr., A 2004;1023:297–303. [PubMed: 14753696]
29. Kempe M, Mosbach K. J. Chromatogr., A 1995;691:317–323. [PubMed: 7894656]
30. Haupt K, Norworyta K, Kutner W. Anal. Commun 1999;36:391–393.
31. Yamazaki T, Ohta S, Yanai Y, Sode K. Anal. Lett 2003;36:75–89.
32. Zhang Z, Liao HP, Li H, Nie L, Yao S. Anal. Biochem 2005;336:108–116. [PubMed: 15582565]
33. Wulff G. Chem. Rev 2002;102:1–27. [PubMed: 11782127]
34. Heilmann J, Maier WF. Angew. Chem., Int. Ed 1994;33:471–473.
35. Alvarez-Lorenzo C, Concheiro A. J. Chromatogr., B 2004;804:231–238.
36. Vidyasankar S, Ru M, Arnold FH. J. Chromatogr., A 1997;775:51–63.
37. Lin JM, Nakagama T, Uchiyama K, Hobo T. Chromatographia 1996;43:585–591.
38. Piletska E, Turner NW, Turner APF, Piletsky S. J. Controlled Release 2005;108:132–139.
39. Chianella I, Lotierzo M, Piletsky SA, Tothill IE, Chen B, Karim K, Turner APF. Anal. Chem 2002;74:1288–1293. [PubMed: 11924591]
40. Turner NW, Whitcombe M, Malecha M, Karim K, Piletska E, Baggiani C, Piletsky S. Biosens. Bioelectron 2004;20:1060–1067. [PubMed: 15556349]
41. Suedee R, Srichana T, Saelim J, Thavornpibulbut T. Analyst 1999;124:1003–1009. [PubMed: 10736857]
42. Armstrong DW, Ward TJ, Armstrong RD, Beesley TE. Science 1986;232:1132–1135. [PubMed: 3704640]
43. Berggren C, Bayoudh S, Sherrington D, Ensing K. J. Chromatogr., A 2000;889:105–110. [PubMed: 10985542]
44. Sellergren B. Makromol. Chem 1989;190:2703–2711.
45. Yu C, Ramström O, Mosbach K. Anal. Lett 1997;30:2123–2140.
46. Turner NW, Jeans CW, Brain KR, Allender CJ, Hlady VH, Britt DW. Biotechnol. Prog 2006;22:1474–1479. [PubMed: 17137293]
47. Hjerten S, Liao JL, Nakazato K, Wang Y, Zamaratskaia G, Zhang HX. Chromatographia 1997;44:227–234.
48. Ou SH, Wu MC, Chou TC, Liu CC. Anal. Chim. Acta 2004;504:163–166.
49. Venton DL, Gudipati E. Biochim. Biophys. Acta: Protein Struct. Mol. Enzymol 1995;1250:117–125.
50. Dhruv H, Pepalla R, Taveras M, Britt DW. Biotechnol. Prog 2006;22:150–155. [PubMed: 16454505]
51. Gu J, Yam CM, Li S, Cai C. J. Am. Chem. Soc 2004;126:8099.

52. Guo TY, Xia YQ, Wang J, Song MD, Zhang BH. Biomaterials 2005;26:5737–5745. [PubMed: 15878379]

53. Shi HQ, Tsai WB, Garrison MD, Ferrari S, Ratner BD. Nature 1999;398:593–597. [PubMed: 10217142]

54. Ramanaviciene A, Ramanavicius A. Biosens. Bioelectron 2004;20:1076–1082. [PubMed: 15556351]

55. Tao Z, Tehan EC, Bukowski RM, Tang Y, Shughart EL, Holthoff WG, Cartwright AN, Titus AH, Bright FV. Anal. Chim. Acta 2006;564:59–64. [PubMed: 17723362]

56. Nishino H, Huang CS, Shea KJ. Angew. Chem., Int. Ed 2006;45:2392–2396.

57. Piletsky SA, Piletska EV, Chen B, Karim K, Weston D, Barrett G, Lowe P, Turner AP. Anal. Chem 2000;72:4381–4385. [PubMed: 11008773]

58. Bossi A, Piletsky SA, Piletska EV, Righetti PG, Turner APF. Anal. Chem 2001;73:5281–5286. [PubMed: 11721930]

59. Rick J, Chou TC. Biosens. Bioelectron 2005;20:1878–1883. [PubMed: 15681209]

60. Rick J, Chou TC. Anal. Chim. Acta 2005;542:26–31.

61. Rick J, Chou TC. Biosens. Bioelectron 2006;22:544–549. [PubMed: 16919439]

62. Pan KM, Baldwin M, Nguyen J, Gasset M, Serban A, Groth D, Mehlhorn I, Huang Z, Fletterick RJ, Cohen FE, Prusiner SB. Proc. Natl. Acad. Sci. U.S.A 1993;90:10962–10966. [PubMed: 7902575]

63. Zhang H, Kaneko K. J. Mol. Biol 1995;250:514–526. [PubMed: 7542350]

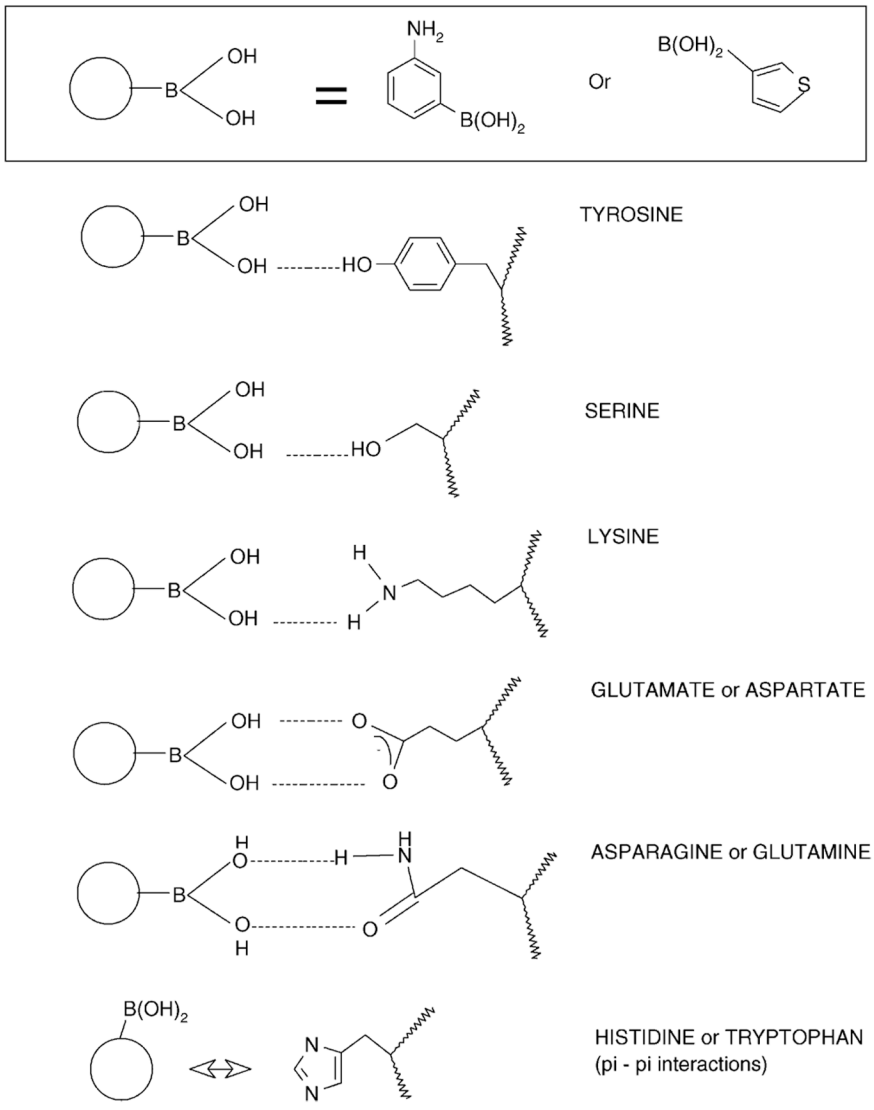

Figure 1.
Possible interactions between APBA monomer and chain groups of amino acids.

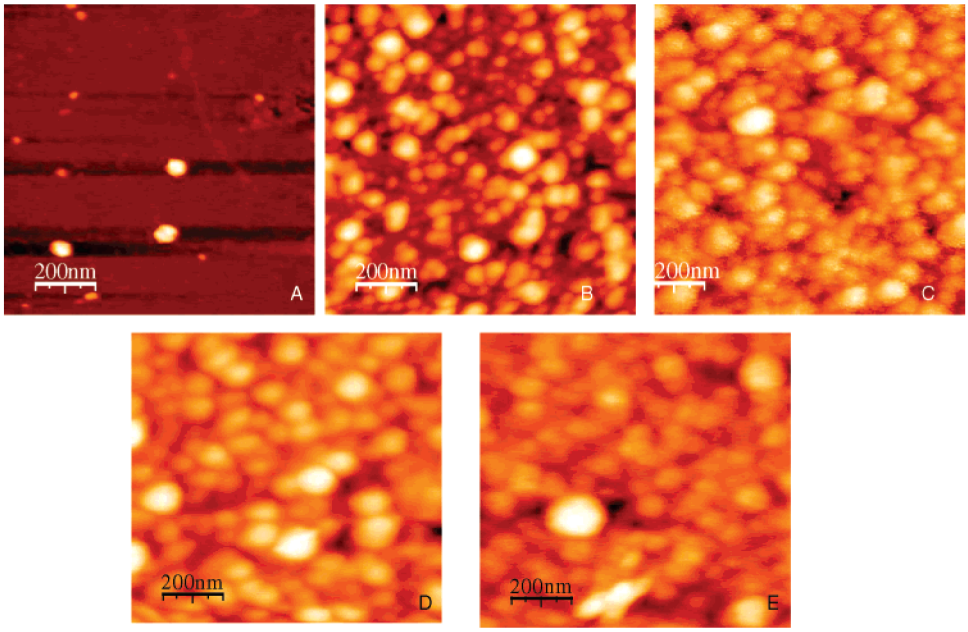

Figure 2.
AFM images of BLG-imprinted poly(APBA) films. Polymerization of each film was stopped after predetermined intervals, and the resultant film was stopped by washing films with 3% acetic acid containing 10 mM Tween 20 at the following times: (A) 2, (B) 10, (C) 30, (D) 60, and (E) 120 min.

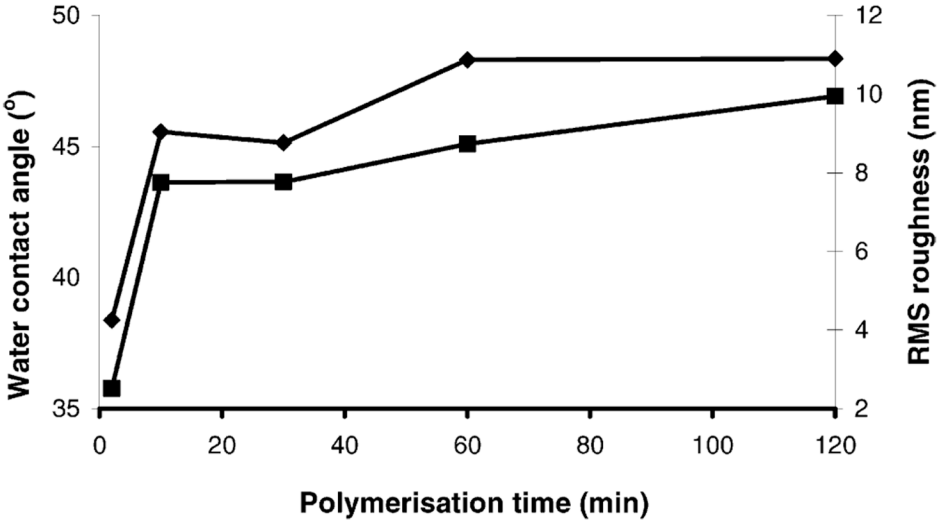

Figure 3.

Water contact angle (left *y*-axis, diamonds) and relative roughness (right *y*-axis, squares) as a function of polymerization time for imprinted poly(APBA) layers on gold surfaces. The clean gold surface had a water contact angle of zero and a surface roughness of less than 1 nm.

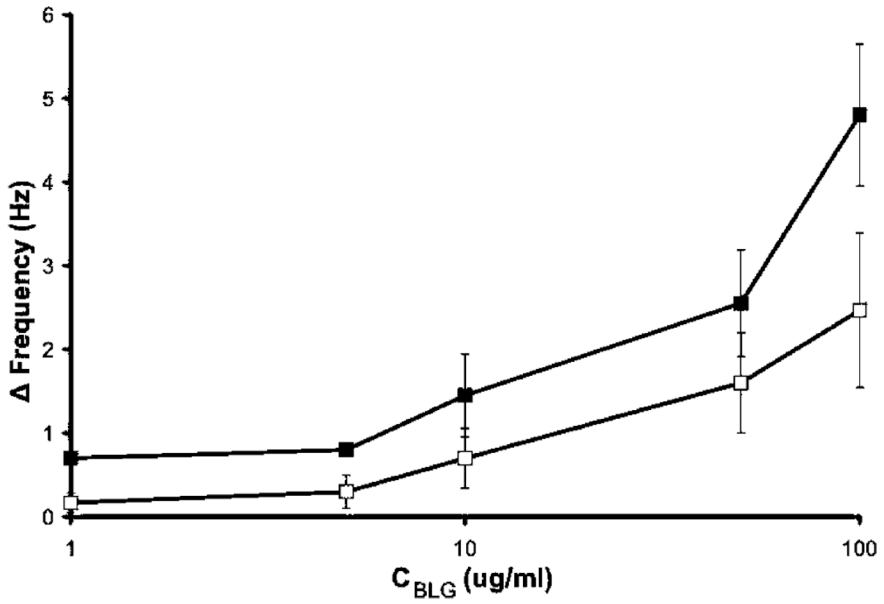

Figure 4.

Rebinding of native β-lactoglobulin (N-BLG) in 50 mM phosphate buffer, pH 7, to poly (APBA) layers imprinted with 0.5 mg mL^{-1} native BLG (closed squares), and nonspecific adsorption to the corresponding nonimprinted poly(APBA) layer (open squares) determined by QCM. Error bars represent one standard deviation, $n = 3$. Some error bars are hidden by point markers.

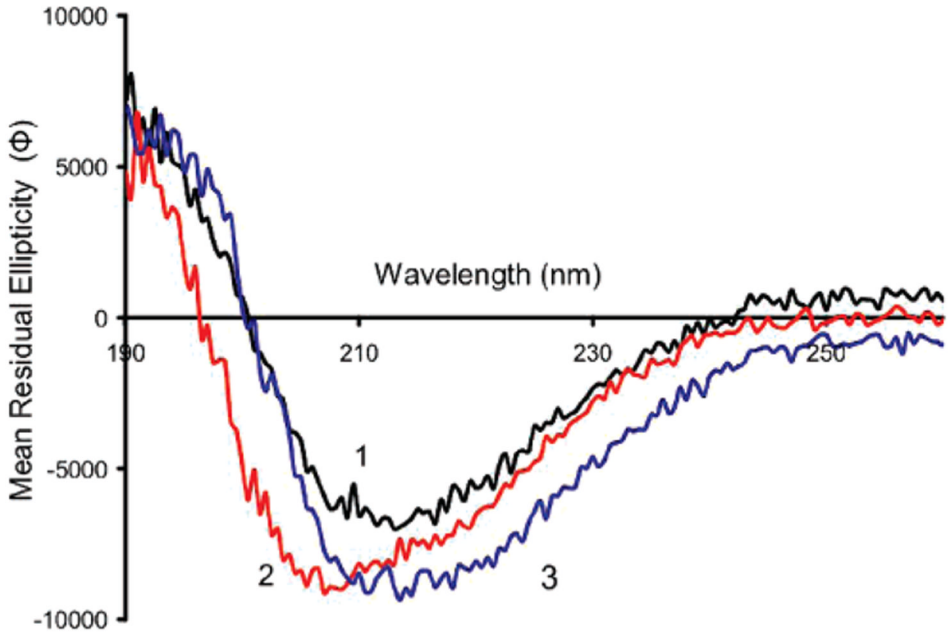

Figure 5.
Circular dichroism spectra of β-lactoglobulin in (1) DDI water (black) (N-BLG), (2) DDI water after heat treatment at 95 °C for 15 min (red) (HT-BLG), and (3) DDI water containing 1% HFIP (blue) (1%HFIP-BLG). Mean residual ellipticity (Φ) is in the units of mdeg cm^2 $dmol^{-1}$.

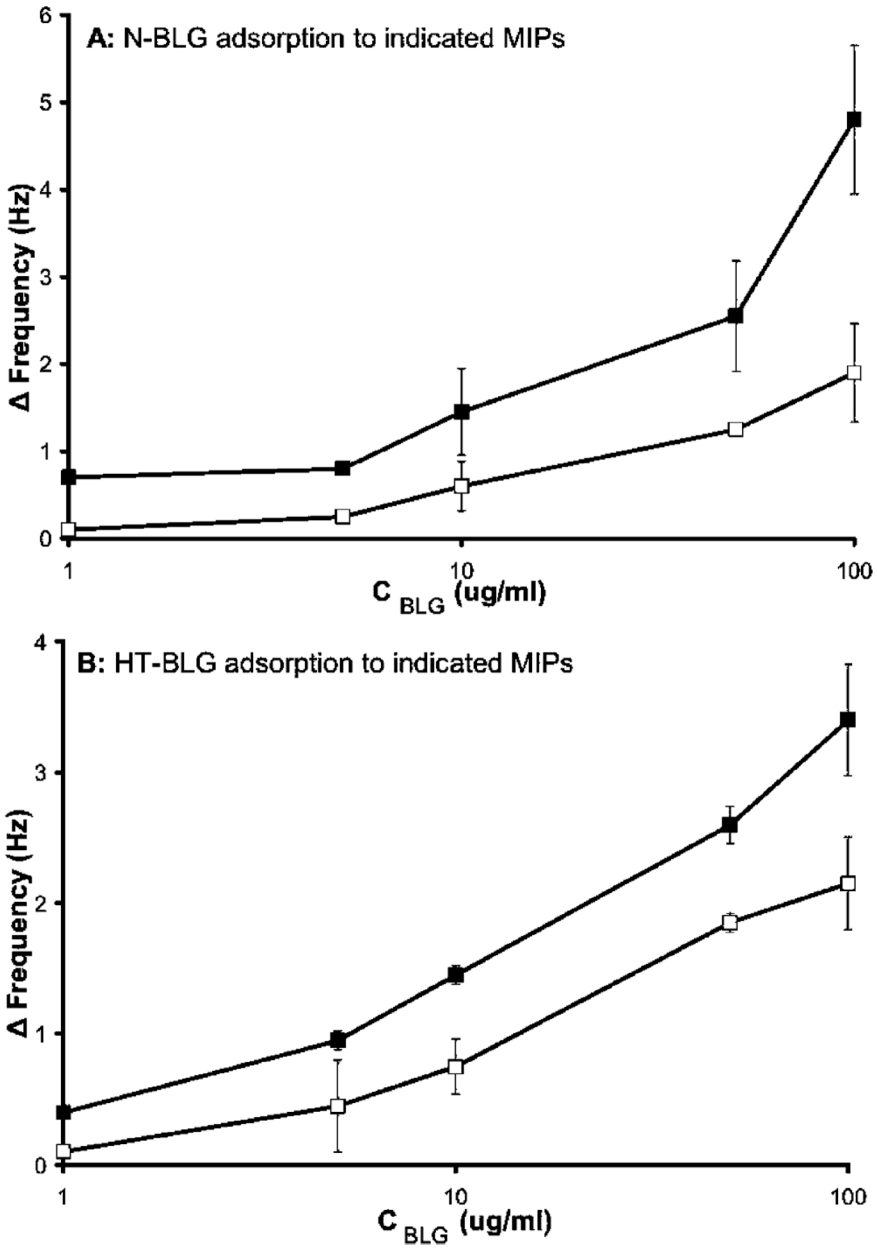

Figure 6.

(A) Native β-lactoglobulin (N-BLG) rebinding to complimentary N-BLG imprints (closed squares), and N-BLG nonspecific binding to HT-BLG imprints (open squares). (B) HT-BLG rebinding to complimentary HT-BLG imprints (closed squares), and HT-BLG nonspecific binding to N-BLG imprints (open squares). Experiments carried out in 50 mM phosphate buffer, pH 7. Error bars represent one standard deviation, $n = 3$. Some error bars are hidden by point markers.

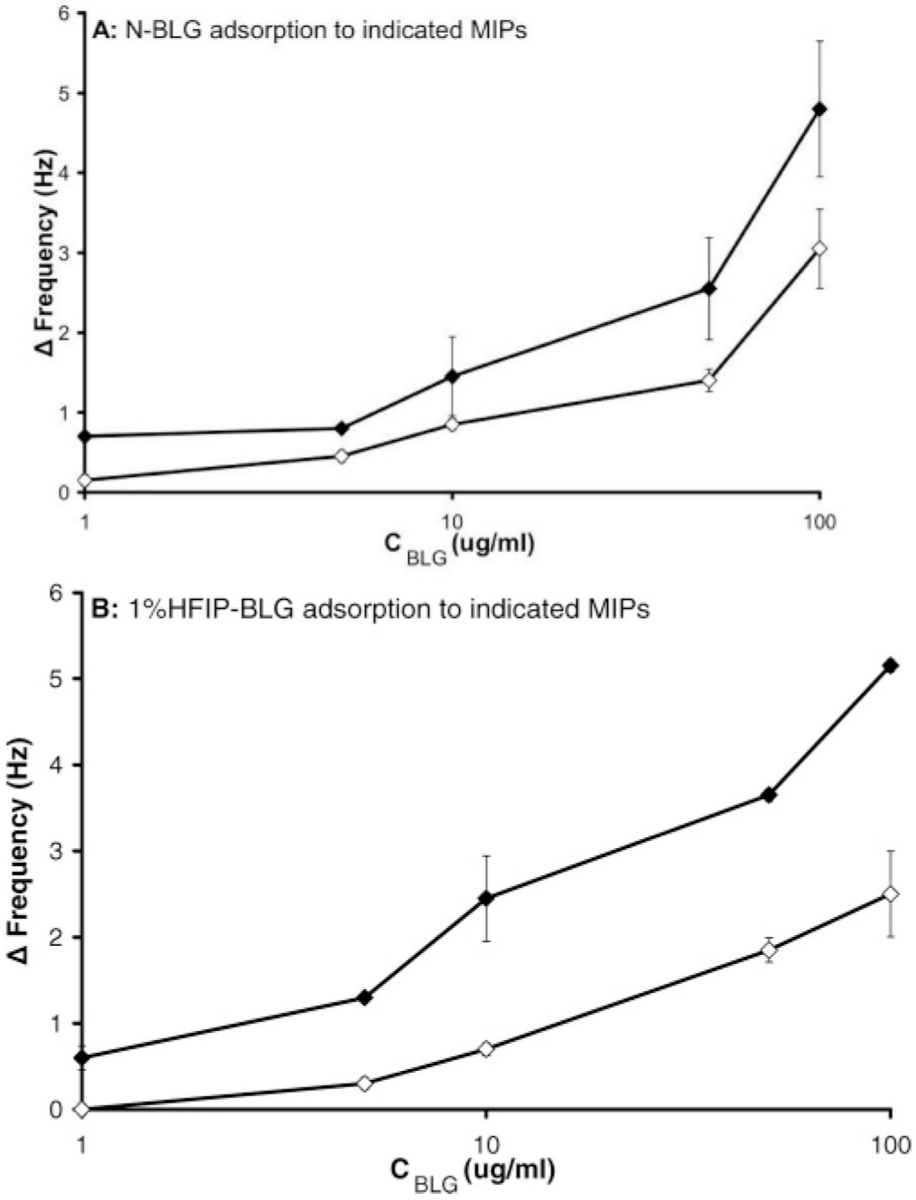

Figure 7.

(A) Rebinding of native β-lactoglobulin (N-BLG) in 50 mM phosphate buffer, pH 7, to N-BLG MIPs (closed diamonds), and nonspecific binding to HFIP-BLG MIPs, also in 50 mM phosphate buffer, pH 7 (open diamonds). (B) Rebinding of HFIP-BLG in 50 mM phosphate buffer + 1% v/v HFIP, pH 7, to HFIP-BLG MIPs (closed diamonds), and nonspecific binding to N-BLG MIPs (open diamonds). Error bars represent one standard deviation, *n* = 3. Some error bars are hidden by point markers.

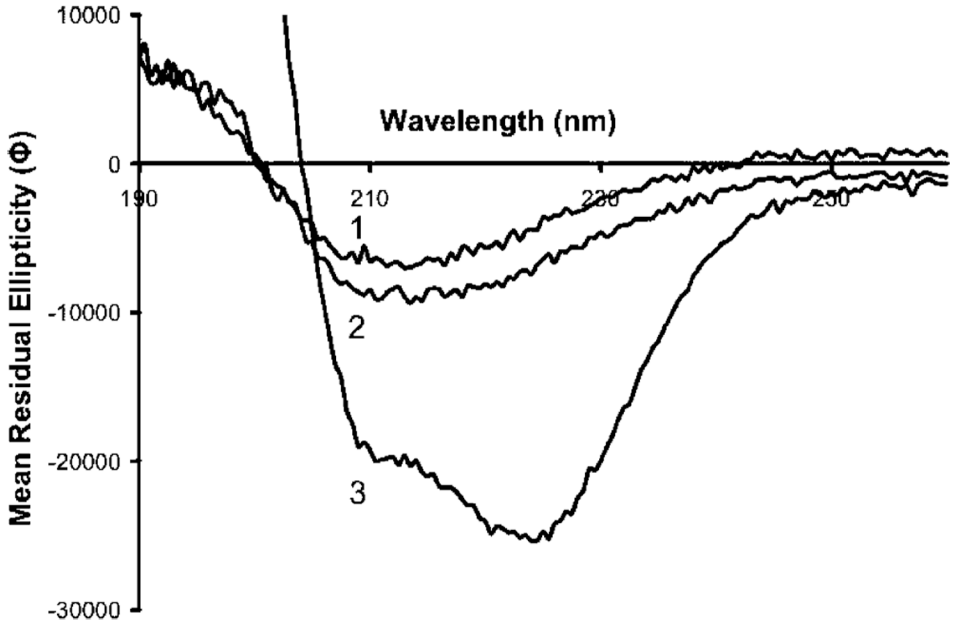

Figure 8.

Circular dichroism spectra of β-lactoglobulin in (1) DDI water (N-BLG), (2) DDI water containing 1% HFIP (1%HFIP-BLG), and (3) DDI water containing 8% HFIP (8%HFIP-BLG). Mean residual ellipticity (Φ) is in the units of mdeg cm^2 $dmol^{-1}$.

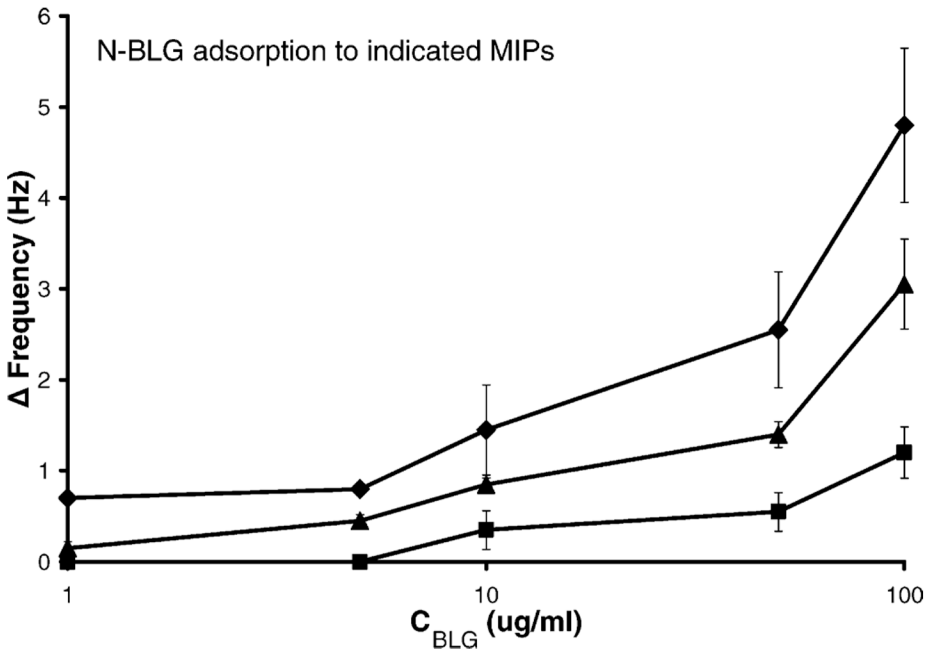

Figure 9.

Rebinding of native β-lactoglobulin (N-BLG) in 50 mM phosphate buffer, pH 7, to an N-BLG MIP (diamonds), to 1% HFIP-BLG MIP (triangles), and to 8% HFIP-BLG MIP (squares). Error bars represent one standard deviation, $n = 2$ for squares and triangles, and $n = 3$ for diamonds. Some error bars are hidden by point markers.

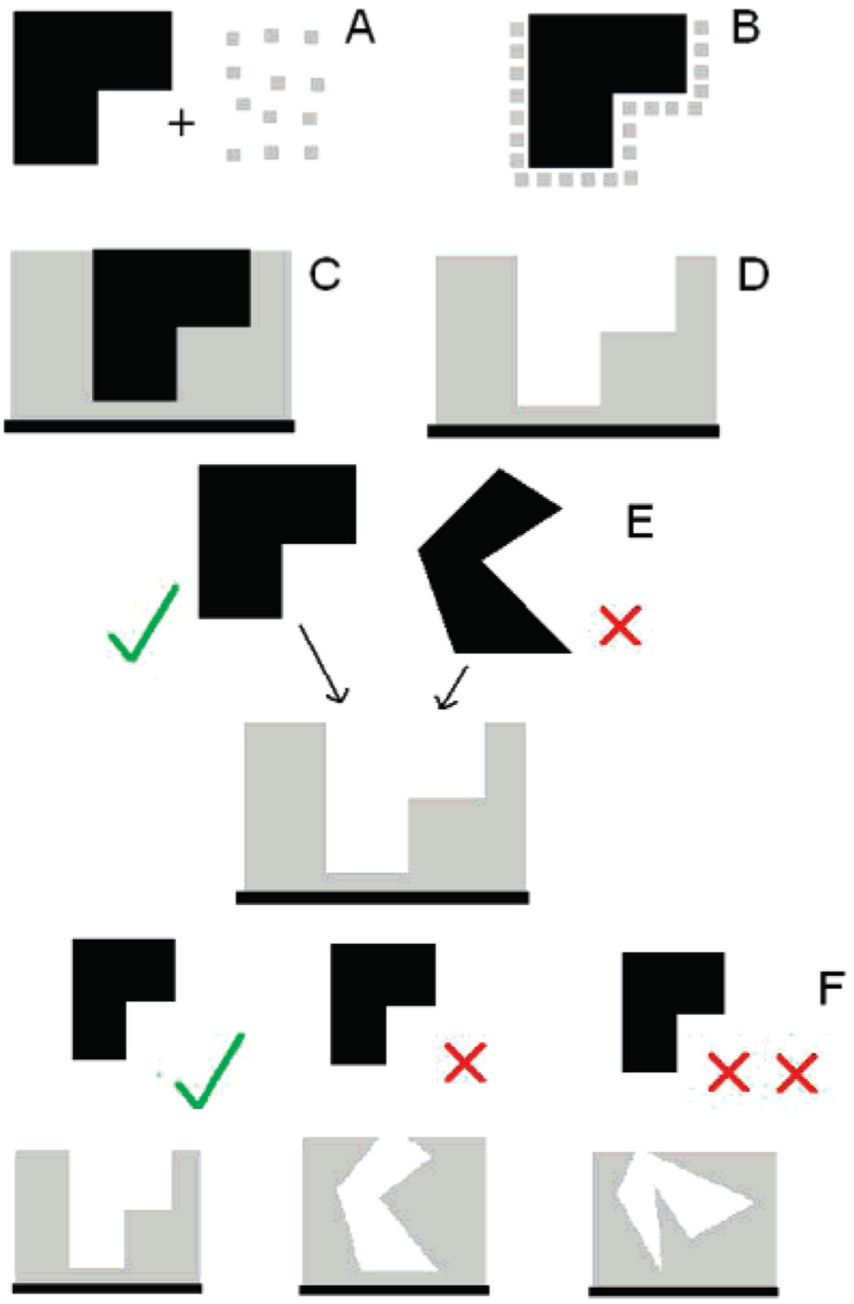

Figure 10.
Schematic representation of conformational protein molecular imprinting on a gold QCM crystal: (A) The template isoform of the protein (black) and APBA (gray) are mixed together to form a complex (B). Upon polymerization this complex is trapped within a poly(APBA) matrix which is adsorbed onto a surface (C). The template protein is extracted (D) to leave an imprint. When challenged with the template isoform or an alternative isoform of the same protein the imprint favors the template (E). The greater the difference between the protein structure used in the imprinting step and that used for rebinding, the less likely it is to bind (F).